Atomic deuterium adsorbed on the surface of liquid helium

Mosk, A.P.; Reynolds, M.W.; Hijmans, T.W.

Publication date
2001

Published in
Physical Review A

Atomic deuterium adsorbed on the surface of liquid helium

A. P. Mosk
Max-Planck-Institut für Kernphysik, Saupfercheckweg 1, D-69117, Heidelberg, Germany

M. W. Reynolds
Creo Products Inc., 3700 Gilmore Way, Burnaby, BC, Canada V5G 4M1

T. W. Hijmans
Van der Waals-Zeeman Instituut, Valckenierstraat 65, 1018 XE Amsterdam, The Netherlands
(Received 7 December 2000; revised manuscript received 21 February 2001; published 29 June 2001)

We investigate deuterium atoms adsorbed on the surface of liquid helium in equilibrium with a vapor of atoms of the same species. These atoms are studied by a sensitive optical method based on spectroscopy at a wavelength of 122 nm, exciting the 1S-2P transition. We present a direct measurement of the adsorption energy of deuterium atoms on helium and show evidence for the existence of resonantly enhanced recombination of atoms residing on the surface to molecules.

DOI: 10.1103/PhysRevA.64.022901 PACS number(s): 34.50.Dy, 67.65.+z, 67.70.+n

Triggered by the first observation of Bose-Einstein condensation (BEC) in atomic gases [1–4], there has been a growing interest in the investigation of quantum degenerate behavior of fermionic atoms. Attention has focused mainly on magnetically trapped gases of the fermionic isotopes ^{6}Li and ^{40}K. The latter isotope was the first atomic Fermi gas to be cooled to below the Fermi temperature [5].

An *a priori* candidate for the comparison between Bose and Fermi gases is the simplest atom of all: hydrogen (H) with its fermionic isotope deuterium (D). The appeal of these atomic gases lies both in the possibility of cryogenic precooling, which enables much larger samples to be cooled than with laser-cooling techniques, and in the existence of a natural two-dimensional quantum gas on the surface of liquid helium. The H quantum gas has been extensively investigated and quantum degenerate behavior (BEC) has been reported both in three dimensions [6] and in the two-dimensional (2d) adsorbed gas [7]. The first optical observation of H atoms in the adsorbed phase was reported in 1998 [8]. In that experiment Lyman-α spectroscopy at a wavelength of 122 nm was used to excite the $1S$-$2P$ transition in a surface-specific way. In this paper we will use Lyman-α spectroscopy to investigate a three-dimensional gas of atomic deuterium in contact with D atoms adsorbed on the surface of liquid helium. Deuterium atoms are easily distinguished from the hydrogen atoms that are always present as impurities because of the large isotope shift of about 630 GHz.

In contrast to H, very few experiments with spin-polarized D have been reported in the literature, mainly because spin-polarized D has been found to be significantly less stable than spin-polarized H and experiments are much harder [9–14]. The key reason for the low stability of D is the high adsorption energy E_a on the helium surface that reduces the overall lifetime because loss processes (molecule formation) occur primarily on the surface. Knowledge of both this binding energy as well as the rate constant governing the formation of molecules are essential ingredients for any experiment aiming at 2d quantum degeneracy. To date the values of both these quantities are not beyond controversy. It has been suggested [14] that the recombination rate on the surface in finite magnetic field may be dominated by a resonant process similar to what was predicted for free D atoms [15]. This assumption has never been properly tested.

The aim of this paper is threefold: first, to provide a direct measurement of the absorption energy of a deuterium atom onto liquid helium, second to determine the rate constant for recombination (molecule formation) of atoms residing on the surface as a function of magnetic field, and finally to attempt to approach the regime of Fermi degeneracy in the adsorbate of D atoms as closely as possible. To be more precise, in this paper we present optical measurements of both the surface gas and the vapor above the surface to extract quantities such as adsorption energy and surface recombination.

The adsorption energy for H on the surface of liquid helium $E_a/k_B = 1.0$ K [11] is well established. For D the values reported in literature vary between $E_a/k_B = 2.6(4)$ K [9], measured in 8 T, and $E_a/k_B = 3.97(7)$ K in zero field [14]. The discrepancy between these values is significantly larger than the accuracy of the measurements. A possible explanation was put forward in Ref. [14]: It is suggested that the presence of one or more Feshbach scattering resonances may influence the measurement of E_a when performed in high magnetic field. In fact, measurements reported in Refs. [9] and [14] rely on the assumption that the ''cross length'' l_{DD} governing the formation of molecules on the surface is independent of magnetic field and temperature. As we will explain below, this assumption may be wrong if Feshbach resonances are present. The measurements of l_{DD} reported in the literature show large variations. For example Hayden and Hardy [13] find $l_{DD} < 30$ Å whereas in Ref. [10] a value of $l_{DD} > 300$ Å was obtained.

It should be noted that an additional complication is the small but finite probability for D atoms to solvate into the liquid helium. With H atoms this solvation probability is negligibly small. For D the chemical potential μ_s for solvation into the liquid corresponds to about 14 K (see Ref. [13]), which is much smaller than for an H atom. Moreover, most

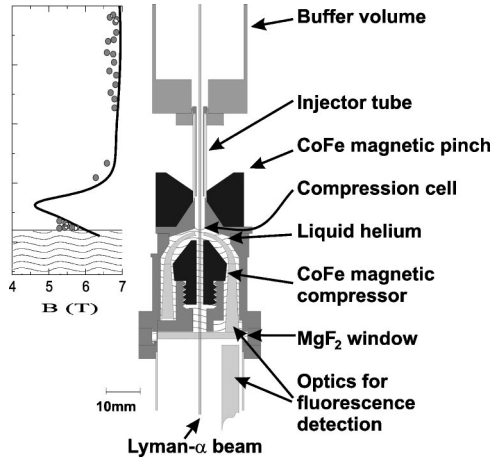

FIG. 1. Drawing of the experimental apparatus. The level of the helium (indicated by wavy lines) and field profile are shown in the left panel. The cell is placed in a 7 T bias field. The magnetic pinch and compressor are cobalt-iron pole pieces producing a pronounced dip (the magnetic barrier) and a local maximum (at the helium surface) in the magnetic field.

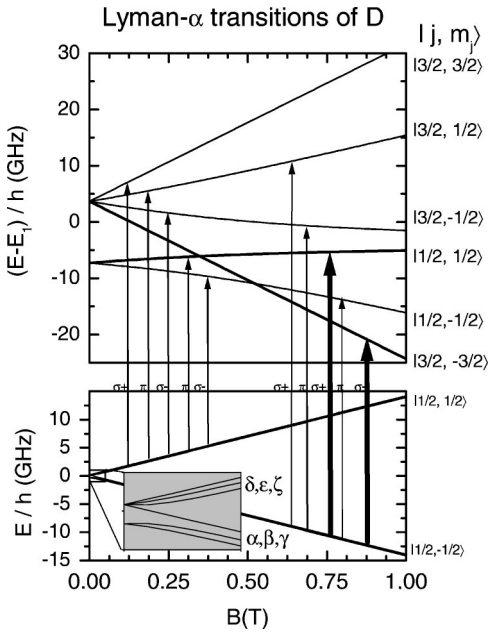

FIG. 2. Level diagram of the $1S$ ground state and $2P$ excited state manifold of D. The measurements are performed in fields between 4 and 8 T. The levels are shown only for relatively low fields in order to keep the hyperfine levels (conventionally labeled α through ζ for the ground state) and the fine structure (for the $2P$ state) visible. The hyperfine splitting of the excited states is much smaller than their natural width. The field values used in the experiment are much larger than the the hyperfine field of the ground-state manifold. Upon optical excitation the nuclear spin is decoupled and so to say ''just goes along for the ride.'' As a consequence, the hyperfine composition of the adsorbed atoms is irrelevant for the spectroscopy. For light propagating along the direction of the applied magnetic field, only two transitions remain allowed in high magnetic field, one σ_+ and one σ_-. These transitions are indicated with thick arrows.

experiments with D atoms to date have been carried out at relatively high temperatures, in the range 0.7 K to more than 1 K. In the present paper the relevant temperatures are below 0.35 K. As the solvation scales roughly as $\exp(-\mu_s/k_BT)$ we can neglect this effect at our temperatures.

All measurements of E_a presented in literature for D atoms are based on a determination of the decay of the atomic gas due to recombination of adsorbed atoms. A direct measurement of E_a has not been performed to date. Such a direct measurement relies on the following simple relation, valid when a three-dimensional gas is in equilibrium with an adsorbed two-dimensional phase in the nondegenerate (Boltzmann) limit,

$$n_2 = n_3 \Lambda \exp\left(\frac{E_a}{k_B T}\right), \tag{1}$$

where n_2 and n_3 are the surface and bulk density, respectively, and $\Lambda = (2\pi\hbar^2/mk_BT)^{1/2}$ is the thermal de Broglie wavelength. To obtain E_a using this equation one needs to have experimental access to n_2 and n_3 simultaneously. Using optical spectroscopy we were able to measure n_3 and to obtain a fluorescence signal proportional to n_2 from the adsorbed atoms.

I. EXPERIMENTAL METHODS

We first describe the experimental setup used for the experiments with H and D adsorbed on He. The heart of this setup is shown in Fig. 1. The apparatus is described in great detail in Ref. [16]. A volume (called the buffer) of approximately 30 cm^3 is filled with D atoms, electron-spin polarized into their high-field seeking states. These are states with electron-spin projection $m_s = -1/2$. From the inset in Fig. 2 it can be seen that there are three such hyperfine states. In fact all three high-field seeking states will be equally populated. The fields are so high (several T, even outside the field range given in the figure) that the electronic and nuclear spins are effectively decoupled. The hyperfine splittings of the excited states are too small to be resolved. Hence, we can without loss of generality suppress the nuclear quantum numbers and consider only spin and orbital angular momentum.

The atoms are produced in a cryogenic discharge in helium vapor operated at a temperature of about 0.8 K. The discharge cell contains solid D_2 on the walls. These molecules are dissociated while the helium discharge is running. The produced monoatomic gas flows towards the buffer volume with a flux of typically $10^{12}-10^{13}$ s^{-1}. We perform experiments while the discharge is running, with the filling flux compensating the recombination losses. With the discharge switched off the D gas decays in a few seconds due to the formation of D_2 molecules.

Below the buffer volume there is a second volume called the cell. The buffer is kept at a higher temperature than the cell to reduce absorption of D on its walls. The atoms adsorb primarily on the surface of a layer of bulk helium, located at the bottom of the cell. The temperature of the liquid helium is about 0.3 K. The buffer temperature is typically between

0.4 and 0.45 K. A strong field gradient (1.6 T/cm) in the cell pushes the atoms towards the helium surface, a principle known as magnetic compression. The cell is separated from the buffer by a magnetic barrier (a local field minimum) that limits the flux of atoms from the buffer to the cell. The cell and buffer are mounted inside the bore of a superconducting solenoid that produces a magnetic bias field of between 4 and 7 T. The magnetic compression and the barrier between buffer and cell are created with cobalt-iron pole pieces (see Fig. 1). We control the flux $\phi_{b\to c}$ from the buffer to the cell by varying the temperature T_b of the buffer volume. The flux is approximately given by

$$\phi_{\mathrm{b}\to\mathrm{c}} \approx \frac{1}{4} n_{\mathrm{b}} \bar{v}_b A_{\mathrm{b}} \exp[-\mu_{\mathrm{B}}(B_{\mathrm{b}} - B_{\min})/k_{\mathrm{B}} T_{\mathrm{b}}], \qquad (2)$$

where $\bar{v}_b$ is the average thermal velocity of atoms in the buffer and μ_{B} is the Bohr magneton. B_{b} and $B_{\min}$ are the magnetic fields in the center of the buffer and at the magnetic barrier, respectively. A_{b} is effective area of the aperture separating the buffer from the cell, which includes the Clausing factor of the tube taking into account the strong magnetic-field inhomogeneity in the barrier region. From a Monte Carlo calculation we obtained $A_{\mathrm{b}} = 1.57\ \mathrm{mm}^2$. The net flux from buffer to cell is $\phi_{\mathrm{b}\to\mathrm{c}} - \phi_{\mathrm{c}\to\mathrm{b}}$ where the back flux $\phi_{\mathrm{c}\to\mathrm{b}}$ is given by the same expression Eq. (2) but with n_{b} replaced by the cell density n_3, B_{b} replaced by the field B_{c} at the bottom of the cell, and T_{b} replaced by the cell temperature T_{c}. The velocity $\bar{v}_c$ is evaluated at the cell temperature T_{c} in this case.

A few words of clarification are needed about the meaning of the cell density n_3. As in Eq. (1) we use the subscript 3 (from three dimensional) for the cell density to distinguish it from the two-dimensional density of atoms adsorbed on the surface. However, in contrast to the buffer where the field is nearly constant, the cell has a field gradient and a concomitant varying density. We will understand n_3 to mean the density just above the surface. The density decreases with height above the surface due to the strong field gradient, analogous to a barometric height distribution. We now introduce a field and temperature-dependent effective volume $V_e = \int_V \exp\{\mu_{\mathrm{B}}[B(\mathbf{x}) - B(\mathbf{0})]/k_{\mathrm{B}}T\} d^3x$. Here the integral is over the volume V of the cell and $B(0)$ is the field at the bottom of the cell (i.e., at the helium surface). V_e is defined such that $n_3 V_e$ equals the number of atoms in the cell.

The atoms in the buffer, the cell, and the adsorbed phase, can all be observed independently using Lyman-α spectroscopy. The light source we used to produce tunable narrow band 122 nm light is described elsewhere [8,17]. As can be seen in Fig. 1 the light beam passes through the apparatus from the bottom to the top. We measure both the absorption of the light as well as the light-induced fluorescence (LIF) as a function of the incident light frequency. The atoms in the buffer are distinguished from those in the cell because they reside in a different magnetic field and the resonance lines experience different Zeeman shifts. The LIF of adsorbed atoms can be distinguished from that of those in the vapor because the resonance lines are shifted by several hundred GHz relative to those of bulk atoms due to the interactions with the liquid helium. Particularly the LIF of the absorbed atoms will be discussed below in more detail.

II. EXPERIMENTAL RESULTS

In this section we discuss the experimental results of spectroscopy of D atoms using Lyman-α spectroscopy. The technique allows us to infer the three crucial parameters in the problem: n_b, n_3, and n_2. The temperatures T_b and T_c are measured directly with resistance thermometers.

In earlier studies with H atoms [8] it was found that the LIF of the surface atoms takes the form of a broad feature shifted about 300 GHz to the red of the spectral line of free atoms in the bulk gas. In the deuterium case the broadening of the surface line is even larger than for H. We have an indication that the fluorescence is broadenend to more than 1 THz. We could not detect a frequency dependence over the 100-GHz lock range of our laser system and the fluorescence was visible when D atoms were present at all frequencies between the H spectrum and a blue detuning of 100 GHz with respect to the D lines. We infer the surface density of D atoms by fixing the frequency of the light to a value close to where the peak of the surface LIF of the D atoms is expected, about 400 GHz to the red of the free-atom resonance. We detect a LIF signal that we assume to be directly proportional to the density n_2 of adsorbed atoms, since we expect temperature or density dependence of the LIF line shape to be negligible in comparison to the 1-THz width. This is based on the observation that for hydrogen atoms adsorbed on either pure ^{4}He or on ^{4}He covered with a (sub)monolayer of ^{3}He, no dependence on temperature was observed. Moreover it was found that the difference in linewidth of the LIF of H on the ^{3}He covered surface was narrower by a factor of about 2.5 as compared to pure ^{4}He substrates. We found that this linewidth scales linearly with absorbtion energy, which for H decreases from 1.0 K to 0.4 K when a layer of ^{3}He is added. If we assume that the scaling continues to hold at least approximately when changing from hydrogen to deuterium, we can infer a linewidth that should be well over than 1 THz. This is indeed too broad to resolve with our apparatus. We have attempted to study D on a ^{3}He covered surface but found that no usable spectra could be taken in our cell due to excessive helium dripping (see caption of Fig. 3), most likely enhanced by the reduced surface tension.

The density n_3 of nonadsorbed D atoms can be measured from the LIF as well as from absorption spectroscopy at frequencies close to the free-atom resonance. This is shown in Fig. 3. The fit to the LIF signal of the bulk atoms is based on a single-scattering model, which is a good approximation at the relatively low densities involved. The small bump in the right wing of the calculated LIF spectrum is due to atoms in the buffer. These atoms are not seen in the experiment, probably because the efficiency of our fluorescence detector breaks down at the very small angles at which these atoms are seen. However the LIF is dominated in any case by the cell atoms that are quite well described by the simple model we used. The model takes into account the Zeeman and Dop-

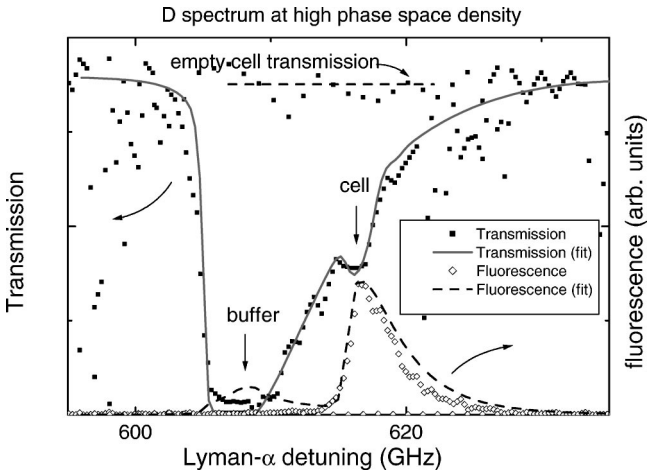

FIG. 3. LIF and absorption spectra for D atoms for the transition between the levels $1S_{1/2}$ $m_s=-1/2$ and $2P_{3/2}$ $m_j=-3/2$, taken with σ_- polarized light. This transition was chosen because it forms a closed cycle and its transition-matrix element is field independent. The full symbols are data of the transmission through the cell and the buffer. The solid line is a fit to the spectrum. The broad saturated feature in the absorption spectrum is due to the buffer atoms and the weaker satellite to the right is due to absorption by the atoms in the cell. The open symbols are the fluorescence due to bulk atoms in the cell. The signal of the surface atoms is not visible in this plot. The noise in the absorption spectrum results from falling He droplets due to the fountain effect caused by the temperature gradient between buffer and cell. The parameters corresponding to the fits are: $n_b \approx 6\times10^{11}$ cm^{-3}, $n_3 \approx 9\times10^{11}$ cm^{-3}. The temperatures are $T_b=0.44$ K, $T_c=0.26$ K. The small discrepancy between the LIF and the fit is explained in the text. The detuning is measured relative to the centroid of the Lyman-α spectrum for H atoms in zero field. This is the average of the transition frequencies to the $J=3/2$ and $J=1/2$ manifolds weighted by their multiplicities (also see Fig. 2).

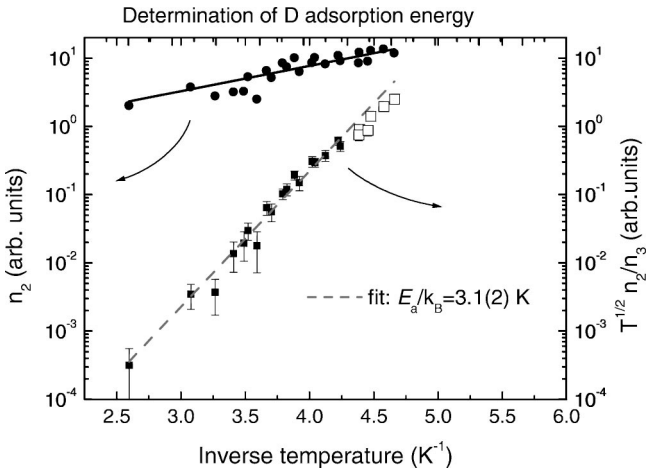

FIG. 4. Measured surface density in arbitrary units (left scale) and ratio of cell density and surface density multiplied by $\sqrt{T}$ in the cell. The data are taken in essentially constant magnetic field of about 6 T. It is permissible to neglect the small variation (about 0.1 T) of the effective magnetic field due to a slightly different distribution of the atoms in the field gradient at different ends of the temperature scale. n_2 varies only weakly in the temperature range shown, the buffer density decreases rapidly with decreasing temperature. The solid points are used in the fit. The open squares correspond to the temperature range where the 2d and 3d systems become thermally decoupled due to fast surface recombination. The fit gives a direct measurement of the binding energy of 3.1 K.

pler effects. The Doppler effect gives rise to a symmetric broadening, which is the same for each atom but its effect is generally not dominant. The Zeeman effect is usually larger and gives rise to an asymmetric inhomogeneous broadening. This is due to the fact the the high-field seeking atoms populate preferentially the region of highest field. The distribution of atoms over different field regions manifests itself as a tail on one side of the line as can be seen in Fig. 3. In fact, for a linear field gradient, this tail reflects the height distribution of atoms above the surface. The height distribution in turn depends on the temperature of the gas in the cell. The shape of the LIF curve is additionally influenced by the solid angle to the detector. Basically the height distribution is weighted by the light-collection efficiency that decreases with height above the surface. As a consequence the tail is more pronounced in the absorption spectrum than in LIF.

The fluorescence detector can be calibrated in an absolute way by comparing the fluorescence peaks with fits to the transmission spectrum, which are essentially exact. From this fit we obtain an absolute value for n_3 whereas n_2 is determined up to a constant factor. We have performed these measurements over a range of temperatures, so that we can use Eq. (1) to directly obtain $E_a/k_B=3.1(2)$ K. The result is given in Fig. 4. The range of temperatures is limited from above by thermal instabilities (fountain effect) of the helium in our apparatus, causing excess noise on the transmission and fluorescence detectors. At the lowest temperatures (for $1/T \gtrsim 4.5$ K^{-1}), there is no thermal equilibrium between the (quickly recombining) adsorbed atoms and the bulk gas, and therefore Eq. (1) is not rigorously valid. We have discarded this temperature region from the fit. In Fig. 4; we also plotted n_2 (in fact we plot the fluorescence signal). It can be clearly seen that the temperature dependence is quite different from that of the ratio n_2/n_3, which indicates that the fluorescence is not a spurious artifact due to bulk atoms.

We can also use Eq. (1) to determine the maximally obtained phase-space density $n_2\Lambda^2$, a measure of how far we are from Fermi degeneracy. Although the measurement of n_2 is not absolutely calibrated, the multiplicative factor follows directly from Eq. (1). We find that at the lowest temperature $T_c=0.19$ K the phase-space density is $\approx 10^{-2}$. In 2d this implies $T_F/T \approx 10^{-2}$ where T_F is the Fermi temperature.

The value of $E_a/k_B=3.1(2)$ K obtained from the fit in Fig. 4 is consistent with the 2.6(4) K measured by Silvera and Walraven [9] but lower than the value 3.97(7) K reported by Arai *et al.* [14]. In the latter paper it is suggested that the difference may be explained by the fact that their experiment is performed in zero field whereas Silvera and Walraven use a field of 8 T. The way in which E_a is measured in both these experiments is by determining the decay rate of the gas. At sufficiently low temperature this decay takes place almost exclusively by formation of molecules from adsorbed atoms on the surface. Consequently the natural way to describe the population dynamics would be in terms of an inelastic cross

length l_{DD} governing the collisions between two adsorbed atoms that lead to the formation of a D_2 molecule. The rate of the process is proportional to n_2 and to the effective surface area A_2 on which the binary collisions take place. This surface is defined analogous to V_e as $A_2 = \int_{\text{surface}} \exp\{2\mu_B[B(\mathbf{x}) - B(\mathbf{0})]/k_B T\} d^2x$, where the integral runs over the surface of the cell. The factor 2 appears in the exponent because two atoms are involved in the formation of molecules. Both V_e and A_2 depend on temperature. Our recombination measurements are performed at $T_c = 0.3$ K. At this temperature we have for our cell: $V_e = 0.015$ cm^3 and $A_2 = 0.14$ cm^2.

The surface density is normally difficult to measure and as a consequence in the literature the decay is usually described in terms of an *effective* bulk-recombination rate constant *K*. If we assume that the gas has no nuclear polarization (equal population of all high-field seeking hyperfine states) we may write [12,14]

$$\dot{N} = -V_e K n_3^2, \tag{3}$$

where $\dot{N}$ is the decay of the 3d gas in the cell. The effective two-body decay rate constant K is given by

$$K = l_{DD} \bar{v} \frac{A_2}{V_e} \Lambda^2 \exp\left(\frac{2E_a}{k_B T}\right). \tag{4}$$

Here $\bar{v}$ is the average thermal velocity of adsorbed atoms. Equations. (3) and (4) are based on the physical picture that atoms spend part of their time on the surface and that in equilibrium, the fraction of particles on the surface is determined by Eq. (1). In the exponent a factor $2E_a$ appears because molecules are formed in pair collisions, hence the process depends on n_2^2. By measuring $\dot{N}$ and n_3 as a function of T one, in principle, obtains values for E_a and K. If one assumes that l_{DD} is independent of B and T one obtains the following relation, given in Ref. [14], between the K in zero field and finite fields larger than the hyperfine field (i.e., for B larger than a few tens of mT):

$$K(0) = \frac{3}{8} K(B)/\varepsilon_D^2, \tag{5}$$

where $\varepsilon_D = a_D/(\sqrt{2}\mu_B B)$ with $a_D/h = 218$ MHz, the hyperfine frequency.

The way just described for determining E_a is plagued by the uncertainty as to whether l_{DD} is in fact independent of B and T. Therefore we have independently measured E_a and l_{DD}. We have measured the field dependence of K in the following manner: The discharge is kept running producing an approximately constant flux of D atoms. Some of the atoms recombine in the buffer volume but most escape over the barrier to the cell. The buffer density is measured by fitting the absorption spectrum of the buffer atoms. From this we calculate the escape flux $\phi_{b\to c}$ from buffer to cell according Eq. (2). From the fluorescence spectrum of the cell we calculate n_3 that gives us $\phi_{c\to b}$, which is generally much smaller than $\phi_{b\to c}$. In steady state the quantity $\dot{N}$ in Eq. (3) is equal to the net flux into the cell $\phi_{b\to c} - \phi_{c\to b}$. From this,

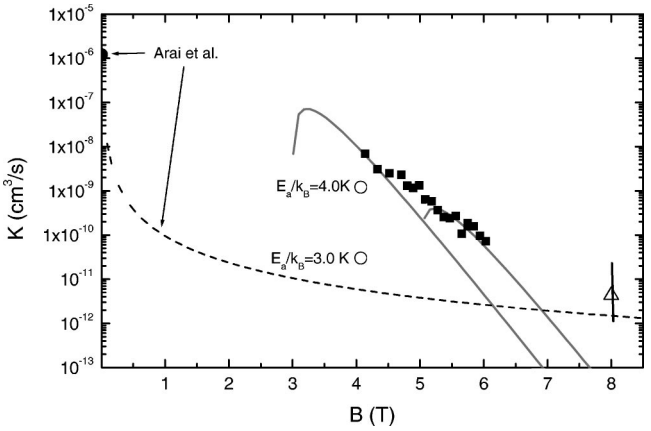

FIG. 5. Rate constant for two-body recombination (full symbols) at $T_b = 0.43$ K and $T_c = 0.30$ K, compared to results from Refs. [9] (triangle) and [12] (open circles). The error margin on the result from Ref. [9] is the result of the extrapolation to our temperature. The solid circle and the dotted line are the measurements of Ref. [14] at zero field and the extrapolation to finite fields, respectively. The solid curves are resonance curves taken from Ref. [15], scaled to appropriate strength and shifted to 3 and 5 T, respectively.

with Eq. (3) we obtain the rate constant K. The result is plotted in Fig. 5 as a function of B.

Since the result may be thought to depend exponentially on thermometry errors, we took the spectra of H that occurs as an impurity in our deuterium simultaneously. Since the H does not recombine quickly, it can be used to check the balance of the fluxes: for H the flux into the cell must equal the return flux. We found the ratio of the density of H atoms in the buffer and the cell to be within the 30% accuracy of the measurement. This indicates that possible thermometry errors (due to, e.g., spurious thermometer magnetoresistance) cannot contribute more than a factor ≈ 2 error to the measured field dependence while the data cover several orders of magnitude over the measured field range.

The conclusion from Fig. 4 that K, or more precisely l_{DD}, depends strongly on B suggests that there may also be a pronounced temperature dependence of l_{DD} at constant magnetic field. This can be checked and the result is already partly contained in Fig. 3. Let us assume for the moment that the net flux from buffer to cell is kept constant. In that case this flux is balanced by recombination on the cell surface and this implies that if l_{DD} is independent of T the surface density n_2 should also be almost independent of T. Clearly we see from the upper curve in Fig. 3 that n_2 is not constant but a decreasing function of temperature. This tentatively suggests a temperature-dependent l_{DD}. To see this more quantitatively we rewrite Eqs. (3) and (4) with the help of Eq. (1) to obtain

$$\dot{N} = -A_2 l_{DD} \bar{v} n_2^2. \tag{6}$$

We now make the assumption that the net flux from the buffer to the cell is equal to the flux of atoms from the dissociator to the buffer. This means that the atoms recombine almost exclusively in the cell rather than on the walls of the buffer. This assumption is reasonable whenever the buffer is significantly colder than the cell and was checked

for cell temperatures below about 0.3 K. Further numerical calculation of A_2 gives $A_2 \sim T$. Hence we have $\dot{N} =$ constant and from Eq. (6) we find $l_{\mathrm{DD}}\bar{v} \sim (Tn_2^2)^{-1}$. From the fit to n_2 in Fig. 3 taken at $B=6.2$ T, we find roughly an exponential dependence of the right-hand side in this equation. We thus find $l_{\mathrm{DD}}\bar{v} \sim \exp(-2E_{\mathrm{act}}/k_{\mathrm{B}}T)$. Here we introduced an the activation energy $E_{\mathrm{act}}/k_{\mathrm{B}}=0.7(3)$ K. If one erroneously would interpret this activation energy as part of the adsorption energy, one finds an apparent adsorption energy: $E_a^* = 3.1(2) - 0.7(3) \approx 2.4(3)$ K in a field of 6.2 T.

III. DISCUSSION

In Fig. 5 we compare our data to values obtained by other groups. The dotted line in the figure is an extrapolation to finite magnetic field of the zero-field measurement of Arai *et al.* [14]. We have scaled their zero-field measurement to correspond to our temperature (the solid dot in Fig. 5). To extrapolate their measurement to finite fields we used Eq. (5). All data compiled in Fig. 5 have been rescaled to correspond to our value of $A_2/V_e = 9$ cm^{-1}. It is clear that our data lie well above the curve of Arai *et al.* Moreover, there is a much stronger dependence on magnetic field. This cannot be due a spurious effect of electron-spin relaxation as for our field range and temperature; this lies many orders of magnitude below our measured range of K values. It was suggested in Ref. [14], on the basis of an analogy with the situation for free D atoms [15], that K may be enhanced in finite field due to Feshbach resonances. Such a resonance occurs when the energy of a highly excited state of the singlet molecule coincides with the energy of a triplet pair of deuterium atoms in the high-field seeking state; the two channels are then coupled by the hyperfine interaction. Near such a resonance we may write K as

$$K_{\mathrm{res}} = \frac{A_2}{V_e}\frac{\Lambda^4}{\tau}\exp\left(\frac{2E_a - 2\mu_{\mathrm{B}}B + E_{\mathrm{D}}}{k_{\mathrm{B}}T}\right). \tag{7}$$

Here E_{D} denotes the dissociation energy of a singlet molecule into a pair of adsorbed atoms. Expression (7) is valid for fields higher than $E_{\mathrm{D}}/2\mu_{\mathrm{B}}$. The reaction time τ characterizes a two-step process: the formation of the excited singlet-state molecule followed by its decay to lower-lying levels.

For free D atoms two Feshbach resonances, 2 T apart, in which the rovibrational levels $(v,J)=(21,0)$ and $(21,1)$ of D_2 are involved, were predicted [15] in field range relevant for this experiment. This suggests that we compare our data with curves corresponding to Eq. (7). Two such curves are plotted in Fig. 5 at the somewhat arbitrarily chosen field values of 3 and 5 T (with the vertical scale adjusted to match the data best). Above a single resonance, the rate will vary proportional to $\exp(-g\mu_B B/k_B T)$. The data vary slightly more smoothly with B. It is to be expected that the free-atom resonances are broadened in the presence of a helium substrate. One might expect a smearing of the same order of magnitude as E_a, which would correspond to a width of more than 4 T, enough to wash out any structure in the resonance spectrum. Another possibility is that motion of the singlet molecule coming off the surface engenders a continuous spectrum of resonances for surface recombination. At any rate the strong observed field dependence supports the idea of resonance recombination.

Three other data points are included in Fig. 5. The measurement at 8 T taken from Ref. [9], extrapolated to $T=0.3$ K using their measured temperature dependence and corrected for our value of A_2/V_e, is consistent with the extrapolation of our data to higher field. The error results from the uncertainty in the value for E_a quoted in Ref. [9], which is reflected in the extrapolation to lower temperature. In fact our data indicate that the influence of the resonance hardly extends to a field of 8 T, which explains why the value for $E_a/k_B = 2.6(4)$ K found in Ref. [9] coincides with ours within the margin of error. The data points at 4.07 T are taken from Ref. [12]. We have extrapolated the measurements taken at their lowest temperature of 0.65 K down to our cell temperature using two different values: 3.0 and 4.0 K, respectively, for the effective adsorption energy (assuming $K \sim T^{-1/2}\exp[2E_a/k_{\mathrm{B}}T]$ for the extrapolation). Both data points obtained in this way from Ref. [12] lie below ours. The reason for this discrepancy is unclear.

In comparing the results of various groups, including the present work, we consistently find marked differences in one or more of the relevant quantities that remain unexplained. Our work does not resolve all inconsistencies and in fact raises new questions. One of the difficulties is that all measurement are performed in either different ranges of magnetic fields and/or temperatures. In addition the underlying assumptions, both in the present work and in the cited literature, are difficult to check and there may be hidden problems with the analysis. One difference is the temperature: our temperature is at least twice as low as in the other measurements. Comparing different measurements requires scaling to the same temperature (or magnetic field). It is not obvious if models used for this scaling always hold. Puzzling is the fact that the binding energy we obtain differs so much from the very accurate value presented for zero field in Ref. [14]. We have no doubt as to the accuracy of those measurements, yet the difference between our data is beyond the combined statistical-error margin. We have no obvious explanation for this discrepancy. We can speculate. First, we note that again the temperature differs by more than a factor of 2. In Ref. [14] it is implicitly assumed that the true binding energy is obtained because the influence of possible resonances is limited to finite-field values and their measurement is done essentially in zero field. Although this argument should hold for the case for free D atoms it is possibly no longer true for adsorbed D atoms. In fact our data in Fig. 4 suggest a much smoother dependence on magnetic field than the underlying picture based on two sharp Feshbach resonances. Such a broadened resonant structure may well extend down to zero field and consequently a temperature dependence of l_{DD} can be present even for vanishing fields, which may account for the apparent discrepancy.

In summary, from our work we conclude that the recombination cross length of D atoms on the surface depends strongly on the magnetic field, which indicates that a reso-

nant recombination process is at work. This also leads to an exponential temperature dependence of the cross length, which was also measured. Such a temperature dependence biased previous measurements of the binding energy of D on liquid He, which explicitly require this temperature dependence to be small. We have performed a direct measurement of the binding energy, which does not rely on recombination processes. In higher field the recombination rate rapidly becomes smaller. Our results indicate that at fields above the resonant region (roughly $B>8$ T) the recombination cross lengths may become sufficiently rather small to make adsorbed D nearly as stable as adsorbed H. Hence one might hope that the interesting configuration of a degenerate, two-dimensional Fermi gas on the surface of a Bose liquid is attainable in this way.

ACKNOWLEDGMENTS

We are grateful to Pavel Bushev, Tycho Sonnemans, and Jook Walraven for fruitful discussions and comments. This research was supported by the Stichting Fundamenteel Onderzoek van der Materie (FOM). Part of the work of A.P.M was supported by the European Commision.

[1] M. H. Anderson, J. R. Ensher, M. R. Matthews, C. E. Wieman, and E. A. Cornell, Science **269**, 198 (1995).
[2] K. B. Davis, M.-O. Mewes, M. Andrews, N. J. van Druten, D. S. Durfee, D. M. Kurn, and W. Ketterle, Phys. Rev. Lett. **75**, 3969 (1995).
[3] C. C. Bradley, C. A. Sackett, J. J. Tollet, and R. G. Hulet, Phys. Rev. Lett. **75**, 1687 (1995).
[4] C. C. Bradley, C. A. Sackett, and R. G. Hulet, Phys. Rev. Lett. **78**, 985 (1997).
[5] B. DeMarco and D. S. Jin, Science **285**, 1703 (1999).
[6] D. G. Fried, T. C. Killian, L. Willmann, D. Landhuis, S. C. Moss, D. Kleppner, and T. J. Greytak, Phys. Rev. Lett. **81**, 3811 (1998).
[7] A. I. Safonov, S. A. Vasilyev, I. S. Yasnikov, I. I. Lukashevich, and S. Jaakkola, Phys. Rev. Lett. **81**, 4545 (1998).
[8] A. P. Mosk, M. W. Reynolds, T. W. Hijmans, and J. T. M. Walraven, Phys. Rev. Lett. **81**, 4440 (1998).
[9] I. F. Silvera and J. T. M. Walraven, Phys. Rev. Lett. **45**, 1268 (1980).
[10] R. Mayer and G. Seidel, Phys. Rev. B **31**, 4199 (1985).
[11] I. F. Silvera and J. T. M. Walraven, in *Progress in Low Temperature Physics*, edited by D. F. Brewer (Elsevier, Amsterdam, 1986), Vol. 10, p. 139.
[12] I. Shinkoda, M. W. Reynolds, R. W. Cline, and W. N. Hardy, Phys. Rev. Lett. **57**, 1243 (1986).
[13] M. E. Hayden and W. N. Hardy, J. Low Temp. Phys. **99**, 787 (1995).
[14] T. Arai, M. Yamane, A. Fukuda, and T. Mizusaki, J. Low Temp. Phys. **112**, 373 (1998).
[15] M. W. Reynolds, M. E. Hayden, and W. N. Hardy, in *Spin Polarized Quantum Systems*, edited by S. Stringari (World Scientific, Singapore, 1989) p. 236.
[16] A. P. Mosk, Ph.D. thesis, Universiteit van Amsterdam, 1999.
[17] O. J. Luiten, H. G. C. Werij, I. D. Setija, M. W. Reynolds, T. W. Hijmans, and J. T. M. Walraven, Phys. Rev. Lett. **70**, 544 (1993).